

## Supporting Information

### Branching Phenomena in Nanostructure Synthesis Illuminated by the Study of Ni-Based Nanocomposites

Liang Qiao<sup>1,2,3,‡</sup>, Zheng Fu<sup>1,4,‡</sup>, Wenxia Zhao<sup>1,5</sup>, Yan Cui<sup>2</sup>, Xin Xing<sup>2</sup>, Ji Li<sup>1,6</sup>, Guanhui Gao<sup>7</sup>, Zhengxi Xuan<sup>1,4</sup>, Yang Liu<sup>1</sup>, Chaeon Lee<sup>1</sup>, Yimo Han<sup>7</sup>, Yingwen Cheng<sup>8</sup>, Shengbao He<sup>2,\*</sup>, Matthew R. Jones<sup>3,7,\*</sup>, Mark T. Swihart<sup>1,4,\*</sup>

<sup>1</sup>Department of Chemical and Biological Engineering, University at Buffalo (SUNY), Buffalo, NY 14260, United States.

<sup>2</sup>Division of Fundamental Research, Petrochemical Research Institute, PetroChina, Beijing 102206, China

<sup>3</sup>Department of Chemistry, Rice University, Houston, Texas 77005, United States.

<sup>4</sup>RENEW Institute, University at Buffalo (SUNY), Buffalo, New York 14260, United States.

<sup>5</sup>School of Chemistry and Chemical Engineering, Ningxia Normal University, Guyuan 756000, China.

<sup>6</sup>MIT Key Laboratory of Critical Materials Technology for New Energy Conversion and Storage, School of Chemistry and Chemical Engineering, Harbin Institute of Technology, Harbin, Heilongjiang 150001, China.

<sup>7</sup>Department of Materials Science and NanoEngineering, Rice University, Houston, Texas 77005, United States.

<sup>8</sup>Department of Chemistry and Biochemistry, Northern Illinois University, DeKalb, Illinois 60115, United States.

‡ L. Qiao and Z. Fu contributed equally to this work.

## Experimental Section

**Chemicals.** Nickel acetylacetonate ( $\text{Ni}(\text{acac})_2$ , NAA)  $\geq 99\%$  from Acros Organics; 1,2-tetradecanediol (TDD) 90%, dodecylamine (DDA)  $\geq 99\%$ , trioctylphosphine (TOP) 97%, oleylamine (OAm) 70%, oleic acid (OA) 90%, and 1-octadecene (ODE) 90% from Sigma-Aldrich were used as received.

**Characterization.** Transmission Electron Microscopy (TEM) images were acquired with a JEOL 2010 operating at 200 kV, a JEOL 2100F operating at 200 kV, or a Titan Themis S/TEM operating at 300 kV; High-Angle Annular Dark-Field Scanning Transmission Electron Microscopy (HAADF-STEM) images were obtained on the Titan Themis S/TEM; Scanning Electron Microscopy (SEM) images were acquired on a Carl Zeiss Auriga Crossbeam SEM/focused ion beam (FIB) system; Powder X-Ray Diffraction (XRD) patterns were acquired using a Rigaku Ultima IV with Cu K- $\alpha$  source.

**Synthesis of the NBCs.** Precursor (NAA), ligands (OAm, OA, TDD, DDA, and/or TOP), and solvent (ODE) were mixed in a three-neck flask, stirred under argon, heated to  $\sim 110$  °C for 30 min, then heated to and kept at the reaction temperature (280 °C) for a certain duration (90 min). The product was cooled to room temperature, mixed with ethanol to destabilize the colloid, and centrifuged to collect the product. The synthesis parameters of the NBCs discussed in this paper are tabulated in Table S1.

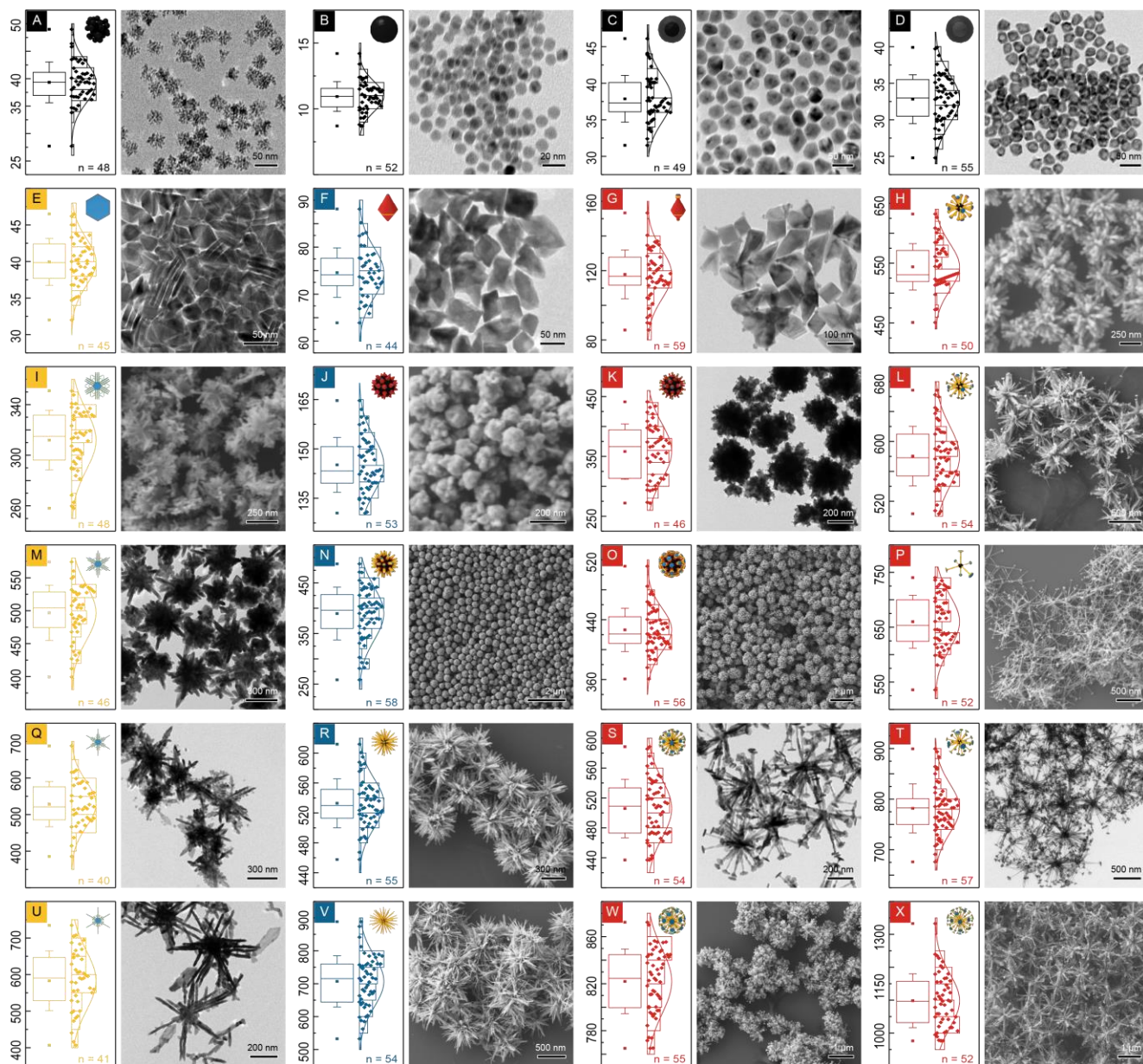


**Figure S 1** Size distributions and wide-area TEM/SEM images of the reported NBCs. (A) clusters; (B) dots; (C) core@shell dots; (D) shells; (E) platelets; (F) polyhedra; (G) polyhedra with stubs; (H) dandelions with bulbs; (I, M, Q, U) dendrites; (J) polyhedral aggregates; (K) polyhedral aggregates with stubs; (N, R, V) urchins; (L, O, P, S, T, W, X) dandelions. 0D dots are labelled in black; 2D dendrites in yellow; 3D urchins in blue; 3D dandelions in red. The unit for the size distribution plot is nm.

In the bar plot for each NBC, the minimum, mean, and maximum are denoted by the solid squares; the 25th percentile, median, and 75th percentile are denoted by the lower, middle, and upper line within the box; the standard deviation is denoted by the lower and upper whiskers (usually beyond the range of the corresponding box).

To determine the size of an NBC in Figure 1, for panels A, B, H, J, K L, N, O, P, R, S, T, V, W, and X, in which the nanostructures' 2D projections appeared circular, the largest end-to-end distance, close to the diameter of its circumscribed circle, of each nanostructure was measured. For panels C, D, F, and G, the largest distance between any vertex and the midpoint of its opposite side was measured. For panels E, I, M, Q, and U, the largest inter-vertex distance was measured.

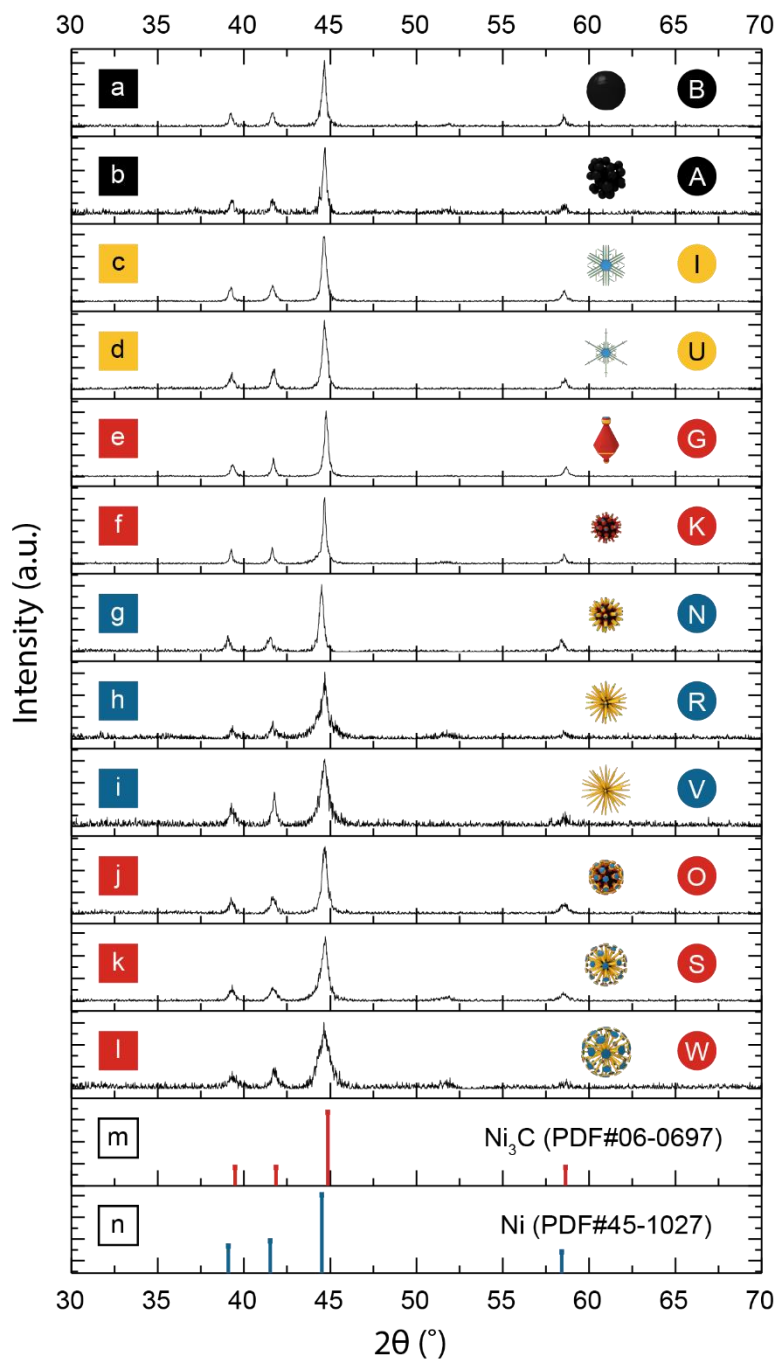


**Figure S 2** XRD patterns of selected NBCs. (a) Dots; (b) clusters; (c, d) dendrites; (e, f) polyhedra and its aggregates; (g, h, i) urchins; (j, k, l) dandelions; (m)  $\text{Ni}_3\text{C}$  standard (JCPDS PDF #06-0697); (n) Ni standard (JCPDS PDF #45-1027). (The letter on the left indicates the order in this figure; the circled letter on the right indicates the NBC's serial number in Figure 1).

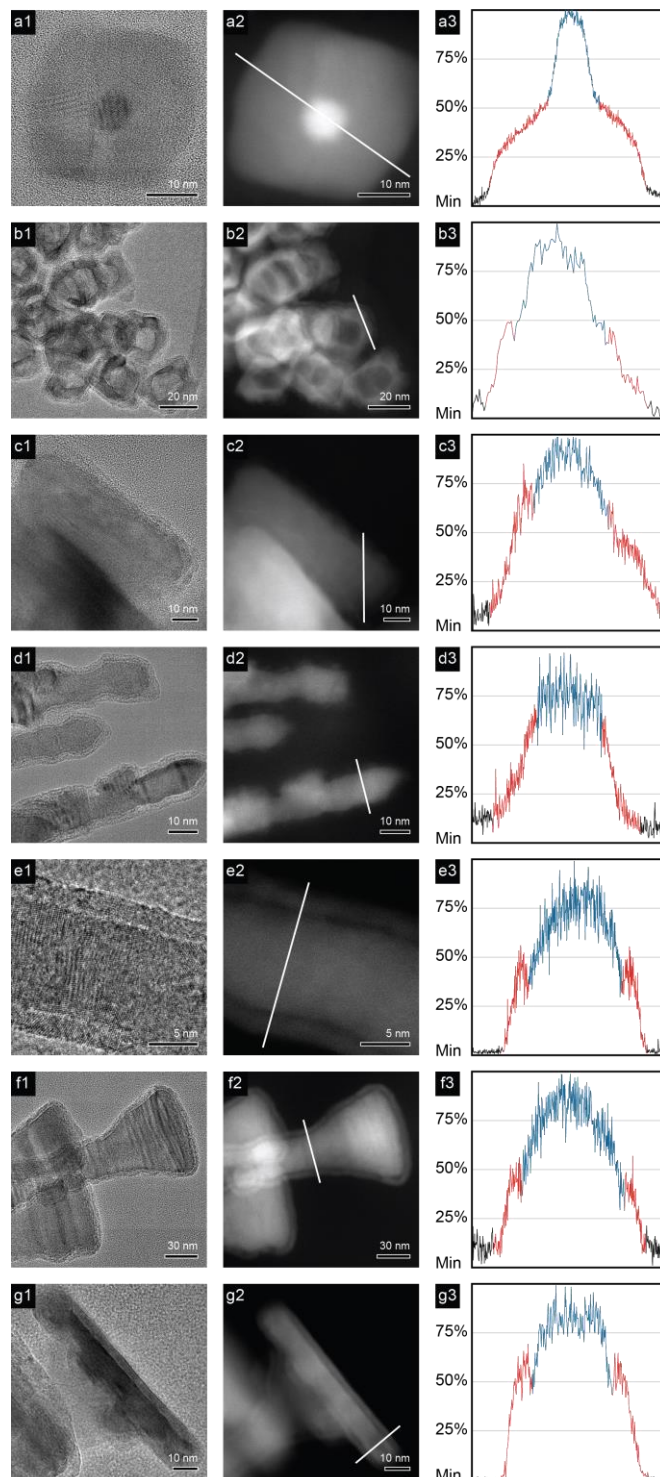


**Figure S 3** TEM images (column 1), STEM images (column 2), and the corresponding contrast profiles (column 3) of various Ni@Ni<sub>3</sub>C nanostructures.

Various NBC nanostructures consistently show a core@shell structure in both TEM (column 1) and STEM images (column 2). Contrast profiles of the parts labeled with white lines in column 2 are plotted in column 3. These profiles more quantitatively show that the contrast of the shell in each NBC (labelled in red) is roughly 50% of that of the core (labelled in blue). Combined with the difference in the *d*-spacings of the core and shell (as discussed in the main text), we can determine that these NBCs are of Ni core@Ni<sub>3</sub>C shell nanostructures.

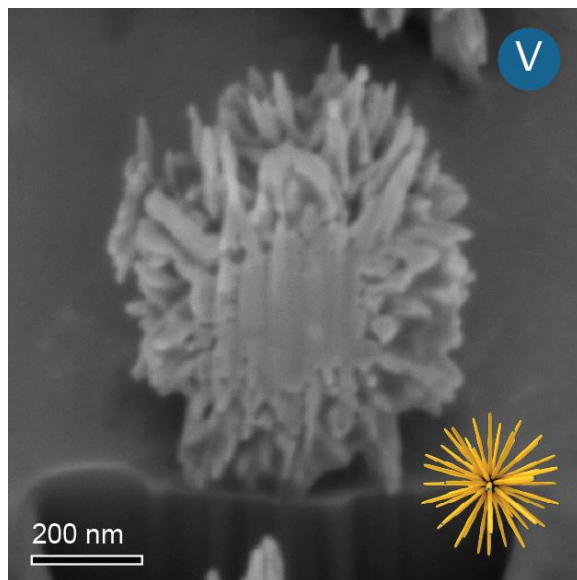


**Figure S 4** SEM image of FIB-milled cross-section of an urchin (Figure 1 V).

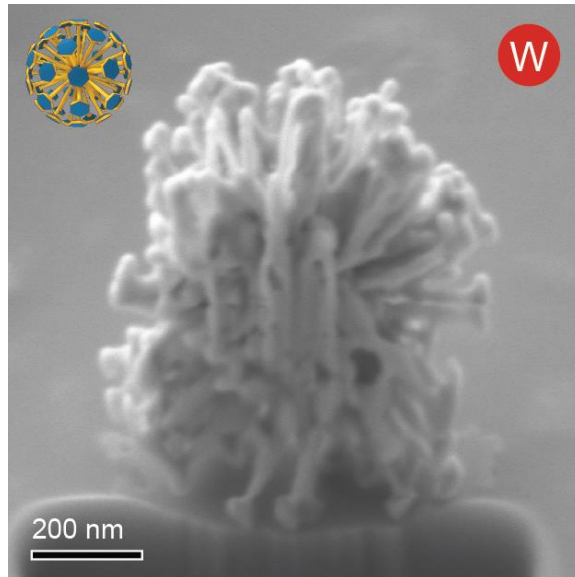


**Figure S 5** SEM image of FIB-milled cross-section of a dandelion (Figure 1 W).